INSTITUT FÜR PLASMAPHYSIK

GARCHING BEI MÜNCHEN

Survey of Studies of Laser Produced Plasmas at the IPP Garching

R. Sigel, S. Witkowski, H. Baumhacker, K. Büchl,
K. Eidmann, H. Hora, H. Mennicke, P. Mulser
D. Pfirsch, H. Salzmann

IPP IV/9 January 1971

Die nachstehende Arbeit wurde im Rahmen des Vertrages zwischen dem Institut für Plasmaphysik GmbH und der Europäischen Atomgemeinschaft über die Zusammenarbeit auf dem Gebiete der Plasmaphysik durchgeführt.

IPP IV/9

R. Sigel, S. Witkowski, H. Baumhacker, K. Büchl, K. Eidmann, H. Hora, H. Mennicke, P. Mulser, D. Pfirsch, H. Salzmann

SURVEY OF STUDIES OF LASER PRODUCED PLASMAS AT THE IPP GARCHING

(January 1971)

ABSTRACT

A status report of November 197o on experimental and theoretical studies of laser produced plasmas at the IPP is given. Experimental investigations of plasma production by nanosecond laser pulses from targets of solid hydrogen and deuterium, of Raman scattering from these materials and of plasma production by picosecond laser pulses are described. The theoretical part comprises numerical studies of the expansion of a two-temperature plasma ($T_e \neq T_i$) and of a multicomponent plasma and also calculations of the fusion rate of an inertially confined plasma.

EXPERIMENTAL INVESTIGATION OF PLASMA PRODUCTION BY NANOSECOND LASER PULSES

The main effort of the group working at Garching in the field of laser produced plasmas has been directed during the last year towards achieving higher laser intensities than available hitherto. The results obtained earlier /1,2/ were obtained with a relatively small ruby laser only. A neodymium glass laser with several amplifiers has now been installed. This system was designed and built at our Institute.

The laser is Q-switched by means of a rotating mirror. It has three amplifiers and is capable of delivering an energy of 1oo J within 25 nsec, i.e. a power of 4 GW. The experiments reported below were performed, however, with an energy of 3o J for 3o nsec only, corresponding to a power of 1 GW.

The diagnostic arrangement used in the experiments is shown in Fig. 1. The pulse shape of the incident laser pulse, the laser light reflected at the target, part of it being reflected from the last amplifier rod, and that of the laser light transmitted by the target were measured with fast photodiodes and displayed on one oscilloscope for each shot. The temperature of the plasma was measured by the well known absorber method using the soft X-ray emission of the plasma. Four plastic scintillators, each covered with beryllium foils of different thicknesses were mounted in the wall of the vacuum chamber. They were arranged close together on a single flange with a diameter of only 2 cm. These small dimensions were possible because the light from the scintillators was guided by light pipes to the multipliers. The time of flight of the ions from the target to the walls of the chamber as well as their angular distribution in space could be measured by a set of probes. At every shot the whole set of diagnostics was used. Discs of solid hydrogen and solid deuterium were used as targets (see Fig. 2). The diameter of these discs was 2 mm, the thickness usually 1 mm. The vacuum in the chamber was about $1o^{-6}$ torr. The laser was focused into the centre of the disc.

Performance of the laser suffers under the action of the laser light reflected at the target and amplified back through the laser. As an extreme example the shape of the laser pulse with and without target is shown in Fig. 3. This picture was taken at an early stage of the experiment with the laser consisting of the oscillator and one amplifier only. The upper trace shows the incident, transmitted and reflected laser light with no target present. The small "reflected" signal was caused by stray light. With the hydrogen target the original pulse with an average power of about 1oo MW is covered by a sequence of intense light pulses which reach well into the gigawatt range. They are out of scale and do not appear very bright on the photograph. As the repetition frequency of these spikes corresponds to the round trip time from the target to the oscillator and back, we may conclude that a single pulse bounces back and forth between target and laser, always being partly reflected at the target. No transmitted light is seen since the target becomes opaque under irradiation. The reflected light, however, shows the same behaviour as the incident light. No further pulses occur after approximately 5o nsec since the laser has created a hole in the solid hydrogen disc, so that the pulse is transmitted and no further reflections can occur.

When the laser was extended to its full length of approximately 7 m, the round trip time was about 4o nsec and hence too long for a single pulse, bouncing between oscillator and target, to build up before the target was destroyed. However, reflection also occurs. The reflected pulse comes back towards the end of the pulse. In Fig. 4 only incident and reflected laser light is shown.

Let us now discuss the results of the temperature measurements obtained from the radiation emission of the plasma in the X-ray region. Four photomultipliers, each with its own absorber and scintillator, were installed and used simultaneously for each shot. This was done mainly for two reasons. Firstly, evaluation of the signals obtained is based on the assumption that the energy distribution function of the electrons in the plasma is Maxwellian. If this is not the case, the use of only two photomultipliers could involve large errors which would not necessarily be noticed in the course of the experiment. With four multipliers the presence of a Maxwellian distribution function may be controlled to a certain extent.

Secondly, with a larger number of multipliers, the temperature can be determined over a wider range with good accuracy.

The absorbers used were beryllium foils with a thickness of 1/1ooo" - 8/1ooo". From the four channels it is possible to determine six intensity ratios and hence six temperatures, which, of course, should all be equal for a Maxwellian plasma. This however, is not the case. The temperatures strongly vary as a function of the foil thickness. They increase from about 2oo eV to about 8oo eV with increasing foil thickness for hydrogen as well as for deuterium.

To check the results for errors, e.g. in calibrating the arrangement or in evaluating the X-ray signals, we replaced the hydrogen target by a carbon target, taking care not to alter anything else in the arrangement. The results are presented in Fig. 5. The abscissa chosen is the cut-off frequency of the various foils. Because the frequency range measured with the various absorber foils is an integral from the corresponding cut-off frequency to infinity, we measure with the thinnest foil in the electron energy range above 15oo eV and with the thickest foil above 28oo eV. As ordinate the various intensities as related to the signal of the photomultiplier with the thinnest foil are plotted on a logarithmic scale. In this representation, as can be shown, the various experimental points should lie, for a Maxwellian electron energy distribution on curves describing approximately straight lines. The inclination of these straight lines decreases with increasing temperature. In the case of carbon the experimental points as determined at the two different power levels used arrange themselve quite reasonably along two lines corresponding to 12o eV and 16o eV.

Thus, in the case of carbon the energy distribution seems to be Maxwellian. Furthermore, the increase of temperature with power corresponds to the dependence $\phi^{0.4}$. This is what one expects from theory. The measurements with carbon thus show that the apparatus is reliable. With deuterium as target material no straight line can be drawn through the measured points. This is also the case for hydrogen. From the measurements we see that the deuterium plasma radiates too much in the hard X-ray region. This means that

we have an excess of fast electrons in the tail of the distribution function, compared with a Maxwellian. So far we have no explanation for this observation. Our protocols show, however, that there is a strong increase of X-ray intensity with intensity of the reflected light. Thus, we are led to the conclusion that intense outbursts of hard X-rays occur if the laser light is reflected by the target.

Besides the X-ray diagnostics, a set of probes at negative potential was used (see Fig. 6). These probes collect the ions and repel the electrons. It is then possible by integrating over the halfspace to determine the total number of ions and, from the time of flight, the mean kinetic energy of the ions. The probe, positioned at an angle of 0°, was a fine tungsten wire, embedded in a quartz capillary. The tip of the wire was in the centre of the lens at the inner side of it. With the other probes the ions were collected at the front side of an insulated wire. Careful investigations were made in order to ensure that the probe signals give the correct number of ions.

Before discussing the results obtained with these probes let us briefly summarize how we imagine the interaction of the focused laser beam and a plane solid hydrogen target (Fig. 6; see also Ref. 2). At the beginning of the laser pulse a strongly absorbing layer at the surface forms and a hot plasma is produced. Owing to the high pressure of the plasma, the solid hydrogen is compressed. As solid hydrogen is a material which is very easy to compress, a deep crater forms during irradiation. While the crater deepens, a shock wave similar to a bow shock preceeds the bottom of the crater, where plasma is continuously produced. When the shock front reaches the rear side of the disc it soon breaks up, so that the laser light may pass through the hole in the disc without strong absorption. For a disc 1 mm thick this happens after about 3o nsec.

With the probes it was found that 6o % of the laser energy reappears as kinetic energy of the ions. The amount of light reflected back through the focusing lens was of the order of 5 %. There remains 35 %. We suppose they are mainly transferred to the shock wave.

From a one-dimensional model /3,4/ only 1o % of the incident energy is expected to be transferred to the shock wave. Under our experimental conditions work is also done by the plasma at the walls of the crater, and therefore the amount of energy transferred to the shock wave should be somewhat higher than 1o %.

Raman scattering from solid hydrogen

So far we have talked mainly about the properties of the hot plasma and its production. There are, however, other interesting aspects of the laser-solid interaction, namely the phenomena occurring at the beginning of the laser pulse. When irradiating our discs of solid hydrogen and deuterium with a ruby laser of 3oo MW power and spectrally resolving the light reflected back through the focusing lens, we got the result shown in Fig. 7. Each of the spectra obtained with solid hydrogen and deuterium shows a strong line which is even more intense than the ruby line. For solid hydrogen this line is located at 975o Å, for deuterium at 875o Å. Wavelength calibration was done with a neon lamp. It turns out that the wavelength of these lines corresponds to the Raman-Stokes line excited by the ruby laser in the two materials.

This Raman-Stokes emission was time resolved with respect to the incident laser intensity using two fast photodiodes which were made sensitive to the Raman and ruby light respectively by means of suitable filters. This was done in the backward and forward directions. Quite reproducible results were obtained (see Fig. 8). We found that at the beginning of the laser pulse a pulse of Raman light with a halfwidth of about 5 - 1o nsec travels in the backward direction. At this time the laser intensity is about a factor of 1oo below its final peak intensity. This pulse is immediately followed by a longer one with a halfwidth about equal to that of the laser pulse. We have denoted this pulse as a Brillouin pulse, which means that we suppose that it is created by stimulated Brillouin scattering. Though this may seem somewhat arbitrary because in the measurements we could not discriminate between Brillouin scattered light and reflected laser light, the abrupt onset of this pulse does suggest that indeed an intensity dependent process like stimulated Brillouin scattering is involved,

at least at the beginning of the pulse. In the forward direction the transmitted ruby light shows a much smoother increase with time. Note that the sensitivity of the photodiode is increased by a large factor as compared with that measuring the incident laser pulse. At the moment when the transmitted light intensity decreases abruptly a short Raman pulse is generated which travels in the forward direction. The two Raman pulses are created at about the same time. The light emission from the plasma at that time is still low. Subsequently, it strongly increases and no further Raman pulses are observed. So one may conclude that when the laser intensity exceeds a certain level, plasma production sets in and Raman scattering ceases because the light is now absorbed in the plasma and no longer reaches the inner part of the target, where only molecules are present. Measurements are under way to determine what role such effects play during breakdown in the solid.

THEORETICAL CONSIDERATIONS

So far we have talked about experiments with the laser. Let us now talk about experiments conducted with our computer. In previous numerical calculations /3,4/ we treated the heating and subsequent gasdynamic expansion of a solid irradiated by a laser. In these calculations the whole set of gasdynamic equations was solved for the one-dimensional case with allowance for the local absorption of laser light. Equal temperatures for ions and electrons were assumed. These calculations have now been extended to the range of higher intensities where electron and ion temperature may be different.

In Fig. 9 profiles of T_e and T_i are shown for the case where a plane solid hydrogen target (located at x=0) is irradiated by a laser from the right. The light intensity is 10^{13} W/cm^2 and the wavelength 1 µm. Profiles are given after 5 and 10 nsec. As can be seen, the electron temperature is higher than the ion temperature. The profiles of density, velocity and light intensity, which were also computed, are not shown here.

In Fig. 10 the dependence of the temperatures on the light intensity can be seen. T_e and T_i are the maximum temperatures after a time of 10 nsec. At intensities of 10^{12} W/cm^2 the difference is small; at 10^{13} W/cm^2 T_e is larger than T_i by a factor 1.4.

Another problem of interest in the literature concerns the experimental observation that with a high Z target irradiated by a laser ion species with different charge expand with different velocities. The expansion velocity of the ions with a high charge is higher than that of those with a lower charge. It has been suggested that the different ions separate owing to electric fields produced in the plasma. This suggestion has been examined in a numerical calculation for the plane case. The set of equations is given in Fig. 11.

We have the equation of continuity, one for each particle species, also the momentum equation for the different ions and for the electrons, and the energy equation for electrons and ions. Forces exerted on the ions are the pressure gradient, the electric field E, which acts in proportion to Z, and friction R between the different ion species. The inertial term in the momentum equation for the electrons is set equal to zero because the electron mass is small compared with the ion mass, whereas the acceleration is of the same order of magnitude. The internal energy of the electrons is altered by absorption of laser light, by work done during expansion, and by heat exchange with the ions. The same terms appear in the energy equation for the ions (except absorption of laser light). This set of equations was solved numerically for the case of two ion species, namely singly and doubly charged ions of equal mass. As a result we get profiles of density and velocity (Fig. 12). These profiles were calculated with and without friction. If friction between the ions is neglected, a nice separation between the two different kinds of ions occurs. The doubly charged ions attain a higher velocity than the others. This is not the case if friction is taken into account correctly. No noticeable separation between the ions occurs. Thus it seems that the separation of ions observed in the experiments must be attributed to other causes, such as the effects of the spatial and temp ral structure of the laser spot, ionization effects, and charge exchange effects.

In a plasma of solid density with a temperature of 1o keV the mean free path for elastic ion-ion collisions is 6o μ. As a fusion gain equal to one may possibly be achieved in a sample whose dimensions are not very large compared with this value, the question arises whether the fusion rate may be reduced by the loss of fast ions.

A numerical calculation of the fusion gain G (fusion energy/input energy) for free expansion (inertial confinement) of a plasma was performed on the pessimistic assumption that the fast ions leave the plasma and react only with a probability modified by elastic collisions. The even-point G = 1 is then reached for a D-T plasma with an initial density of $6 \times 1o^{22}$ cm^{-3} at an energy input $E_o = 3.5 \times 1o^7$ joule /5/. A more realistic treatment was based on

a kinetic equation for the distribution function f of a one-ion-type plasma, with the electron dynamics, electron-ion collisions and space charge fields being neglected:

$$\frac{\partial}{\partial t} f + v \frac{\partial f}{\partial x} = \left(\frac{\partial f}{\partial t}\right)_{\text{ion-ion coll.}}$$

The left hand side of this equation vanishes if f depends on the constants of motion $\underline{v}$ and $\underline{x} - \underline{v}t$ only /6/. The collision term is zero for exponential functions of the collision invariants $\underline{v}$ and $\underline{v}^2$, from which as a solution of the full equation a Maxwellian distribution for the velocities and a Gaussian density distribution are concluded. The expression for the fusion rate

$$n^2 \langle \sigma v \rangle = \int d^3 v_1 \int d^3 v_2 \; \sigma(|\underline{v}_2 - \underline{v}_1|) \; |\underline{v}_1 - \underline{v}_2| \; f(\underline{x}, \underline{v}_1, t) \; f(\underline{x}, \underline{v}_2, t)$$

can then be evaluated to the final expression

$$n^2 \langle \sigma v \rangle = \frac{n_o^2}{2} \left(\frac{T(t)}{T}\right)^3 \exp\left[- \frac{2x^2}{R_o^2} \cdot \frac{T(t)}{T} \right] \langle \sigma v \rangle_o$$

where R_o and T_o are the initial values of the plasma radius and temperature. This shows a self-similarity expansion of the plasma - as is well known from the hydrodynamic theory /7/ - with an aidabatic decrease of the plasma temperature T at time t

$$T(t) = T / \left[1 + 2kT_o t^2 / (m R_o^2) \right]$$

where m is the ion mass. Assuming that a similar behaviour also occurs for a D-T mixture, we arrive at

$$\langle \sigma v \rangle_o = \int_o^\infty \sigma(v) v^3 \exp\left(- \frac{\bar{m} v^2}{2kT(t)} \right) dv \Big/ \int_o^\infty v^2 \exp\left(- \frac{\bar{m} v^2}{2kT(t)} \right) dv$$

where $\bar{m}$ is the reduced mass of the colliding particles. This expression does not show any specific effect of the loss of fast ions which can only be found in the time dependence of the density profile. The fusion gain can then be calculated numerically and

yields for the Gaussian density profiles for optimized initial volumes

$$G_{gauss} = 3.93 \times 10^{-18} n_o^{2/3} E_o^{1/3} \quad \text{for D-T}$$

$$G_{gauss} = 1.79 \times 10^{-19} n_o^{2/3} E_o^{1/3} \quad \text{for D-}$$

The even point $G = 1$ is reached at $n_o = 6 \times 10^{22}$ cm^{-3} for $E_o = 4.6$ MJ (D-T) and $E_o = 4.2 \times 10^{4}$ MJ (D-D).

PLASMA PRODUCTION WITH PICOSECOND PULSES

In order to investigate the mechanism of plasma production at very high intensities, a mode-locked laser oscillator with single pulse selection was combined with our amplifier chain. The whole system is shown in Fig. 13. Mode-locking is achieved with a liquid dye cell. The oscillator rod is cut at the Brewster angle and the mirrors are wedged. A single pulse is selected by a Kerr cell positioned between crossed polarizers, the Kerr cell being switched by a laser triggered spark gap. The pulse then passes twice through two amplifiers, the plane of polarization being rotated 90° by a $\lambda/4$ plate. The pulse is then deflected by the Glan prism and amplified by the cascade of amplifiers. The pulse width was determined by the two-photon-fluorescence method. As the protection system which shields the oscillator against reflections from the target had not been installed, the energy of the pulses was kept low, of the order of 1 joule.

A number of shots on targets of solid hydrogen and deuterium were recently made with this system. With single laser pulses for which the two-photon-fluorescence method indicated a pulse width of 1 - 3 picoseconds, unequivocal and reproducible signals of the diagnostic arrangement could be observed. For such pulses X-ray signals indicating a high electron temperature could be observed. If these signals are plotted as in Fig. 5, it is found that they are emitted by electrons with a Maxwellian distribution function with a temperature of about 2 keV. Simultaneously the number of particles and the mean kinetic energy of the ions in the plasma were determined by the set of probes. The total expansion energy of the ions equals the incident laser energy, thus indicating that the major part of the laser energy has been absorbed in the target. This agrees with the observation that less than 10 % of the laser energy was reflected back through the focusing lens. Further investigations that will afford a comparison with theoretical models for plasma heating are now underway.

REFERENCES

1 R. SIGEL, K. BUECHL, P. MULSER and S. WITKOWSKI, Phys. Lett. 26A, 498 (1968).

2 R. SIGEL, Z. Naturforsch. 25a, 488 (197o).

3 P. MULSER and S. WITKOWSKI, Phys. Lett. 28A, 151 (1968).

4 P. MULSER, Z. Naturforsch. 25a, 282 (197o).

5 H. HORA and D. PFIRSCH, 197o Sixth Intern. Quantum Electronics Conference, Kyoto, Japan, 7.-1o.9.197o, p. 1o.

6 H. HORA and D. PFIRSCH, IPP Report IV/7, VI/91 (197o).

7 H. HORA, Laser Interaction and Related Plasma Phenomena, Plenum Press 197o, p. 365.

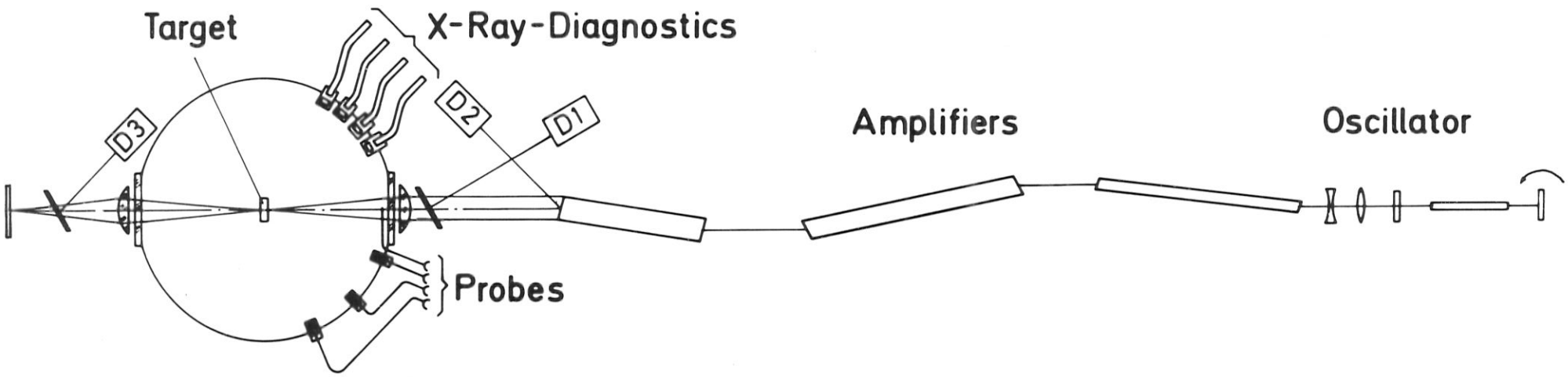

Fig. 1 Experimental set-up.

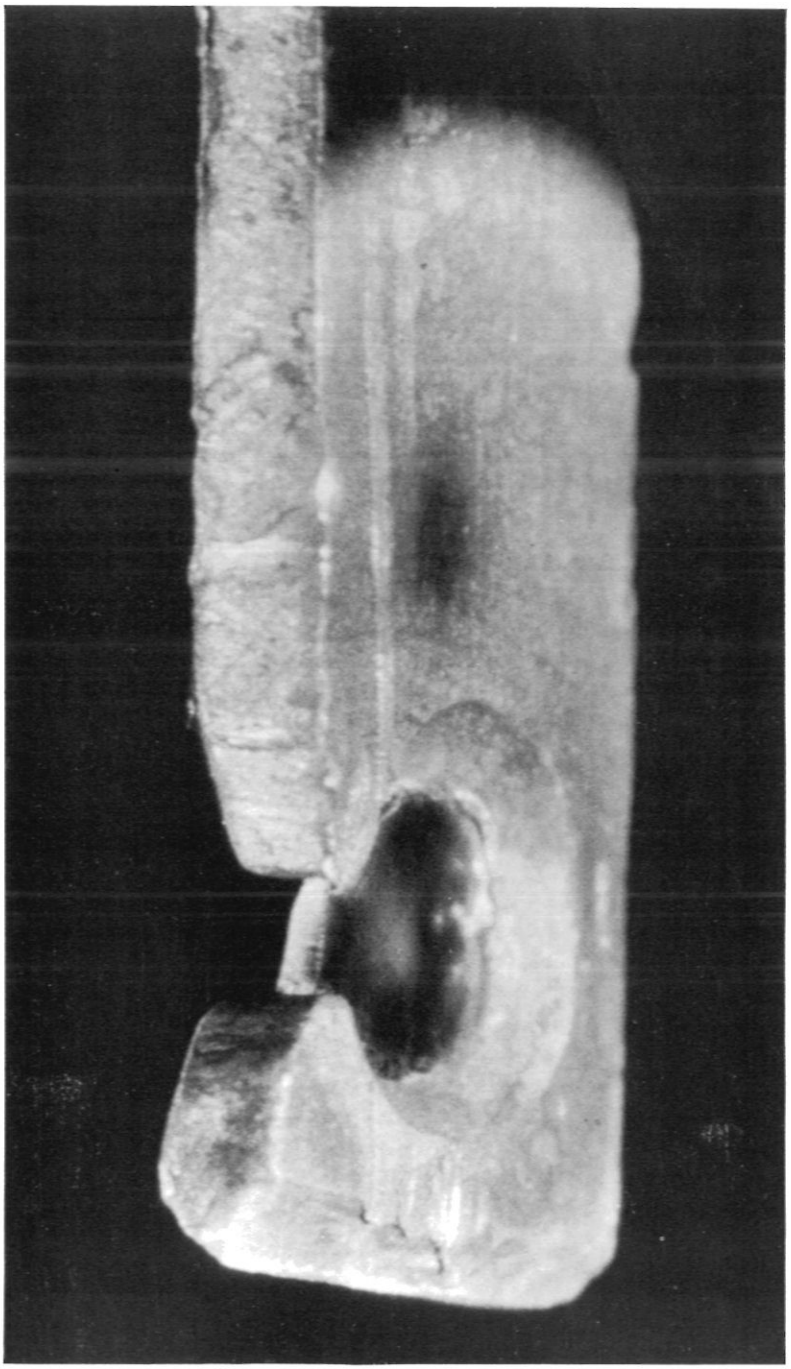

Fig. 2 Cooling finger with disc of solid hydrogen. Diameter of the hole 2 mm. The adjustment laser is focused into the centre of the disc.

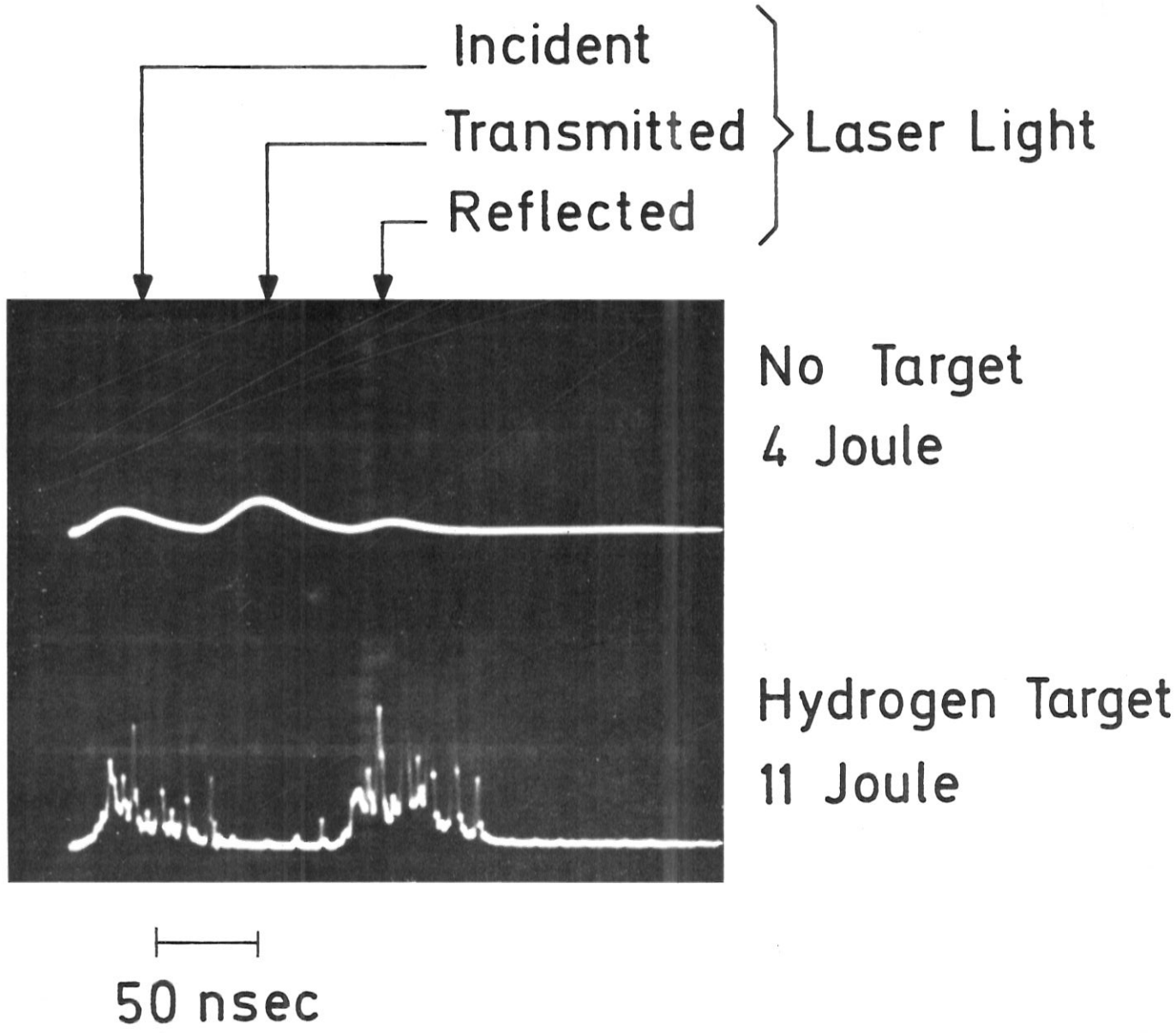

Fig. 3 Oscillograms of the signals of the photodiodes D_1-D_3 without and with target. The laser consists of the oscillator and one amplifier only.

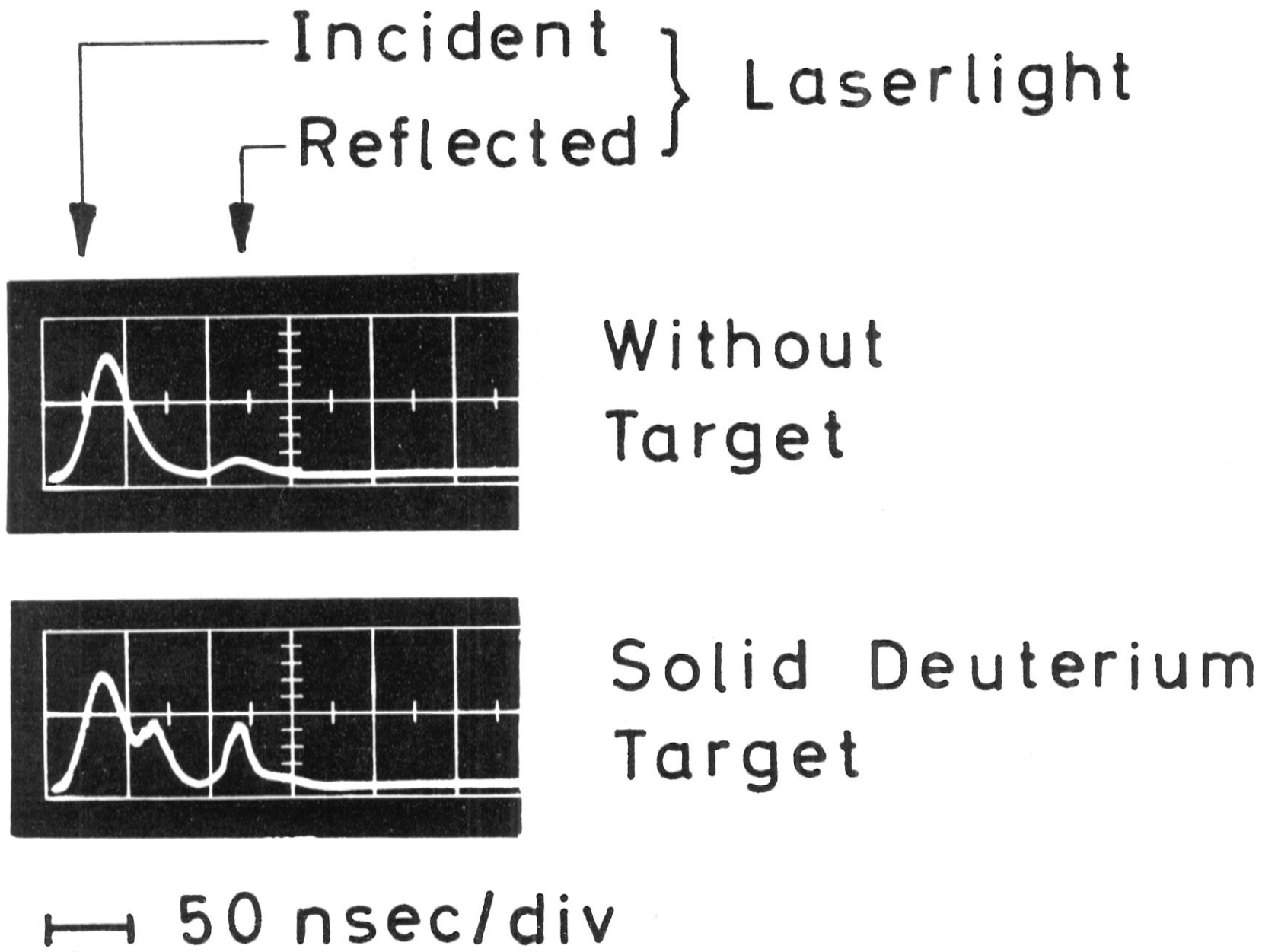

Fig. 4 Oscillograms of the signals of the photodiodes D_1 and D_2 without and with target. Laser as shown in Fig. 1.

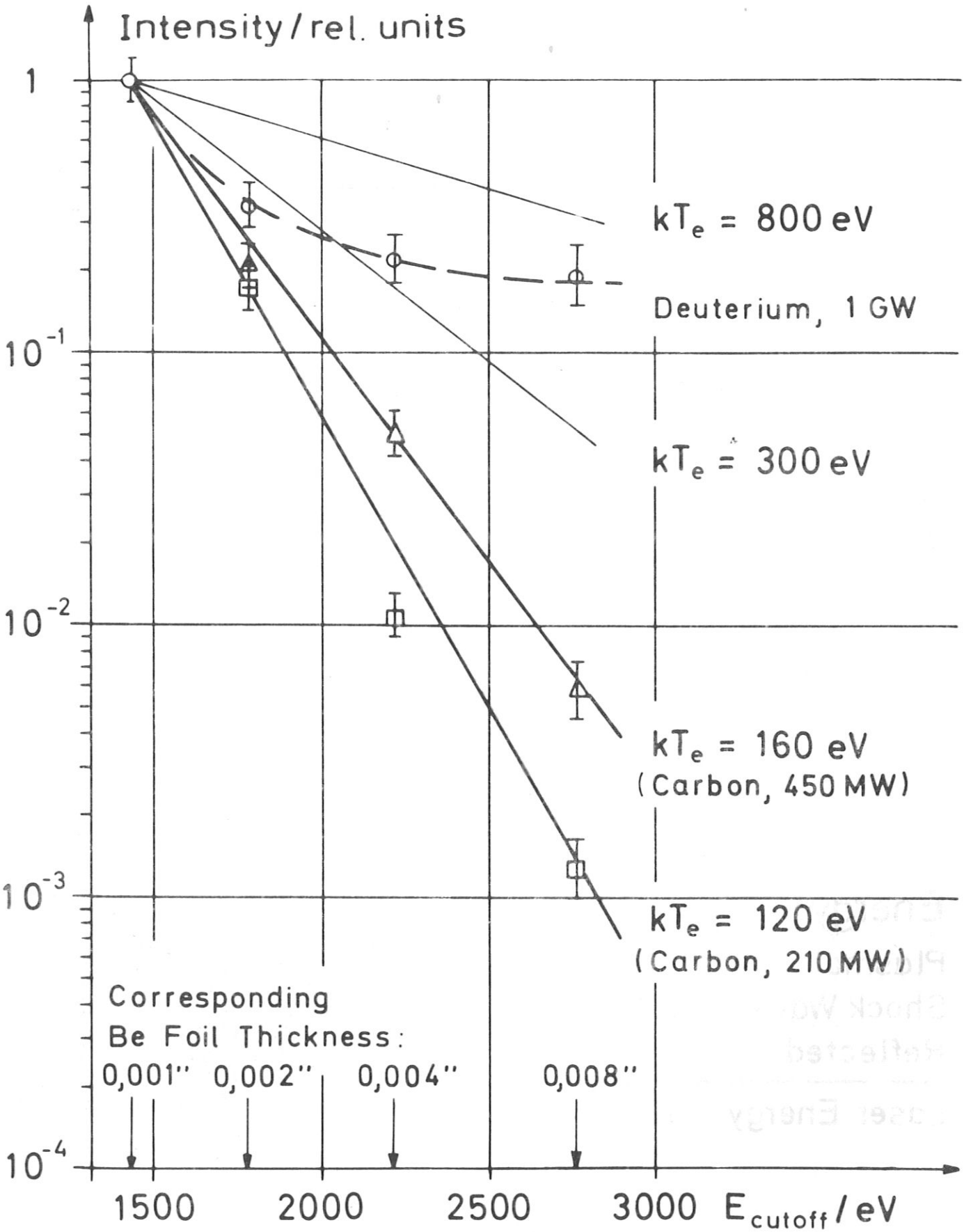

Fig. 5 Intensity of the signals of the various photomultipliers (related to the signal of the photomultiplier with the thinnest foil) versus cut-off frequency of the absorber foil.

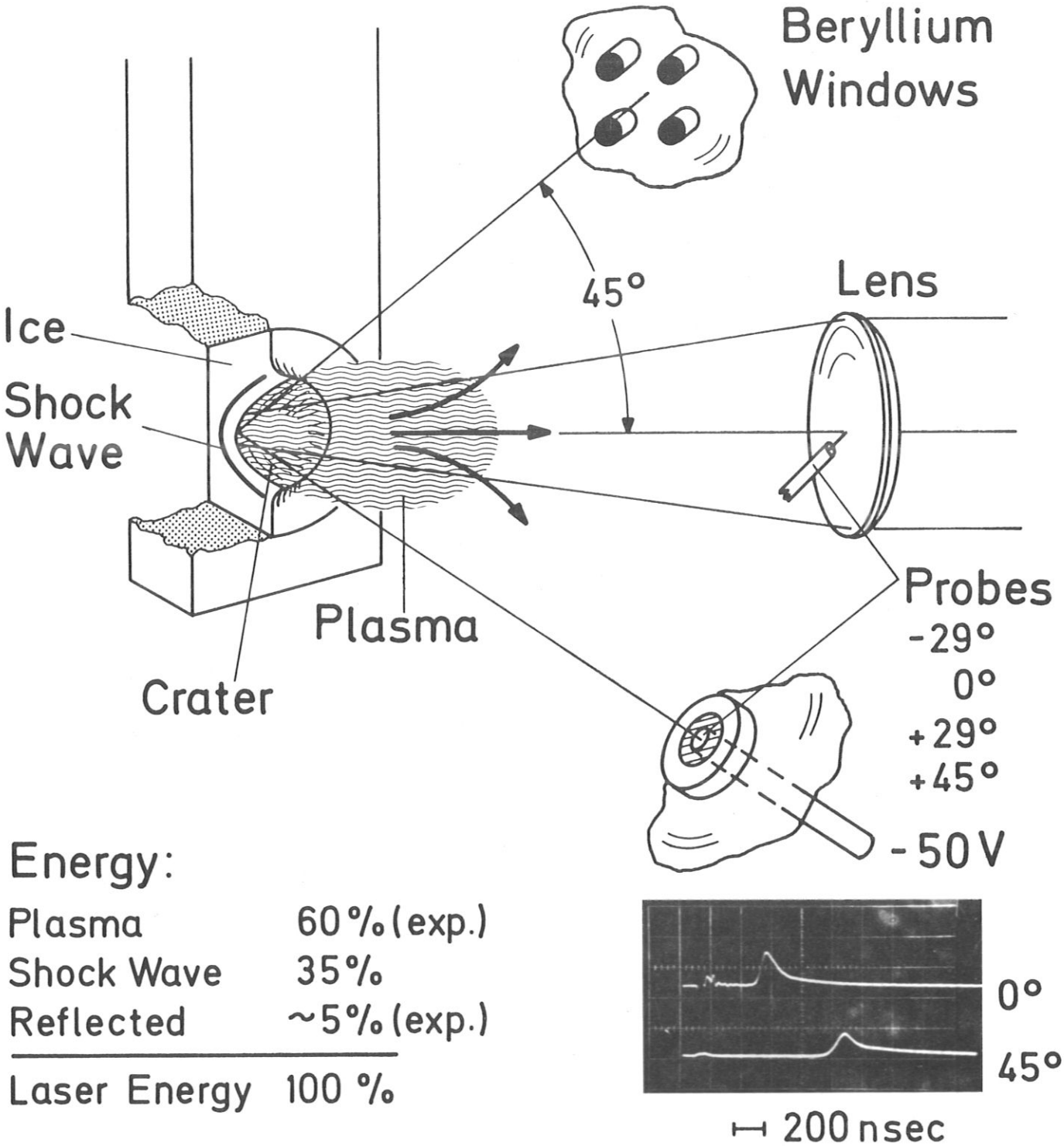

Fig. 6 Diagnostics and interaction of the focused laser beam with the disc of solid hydrogen.

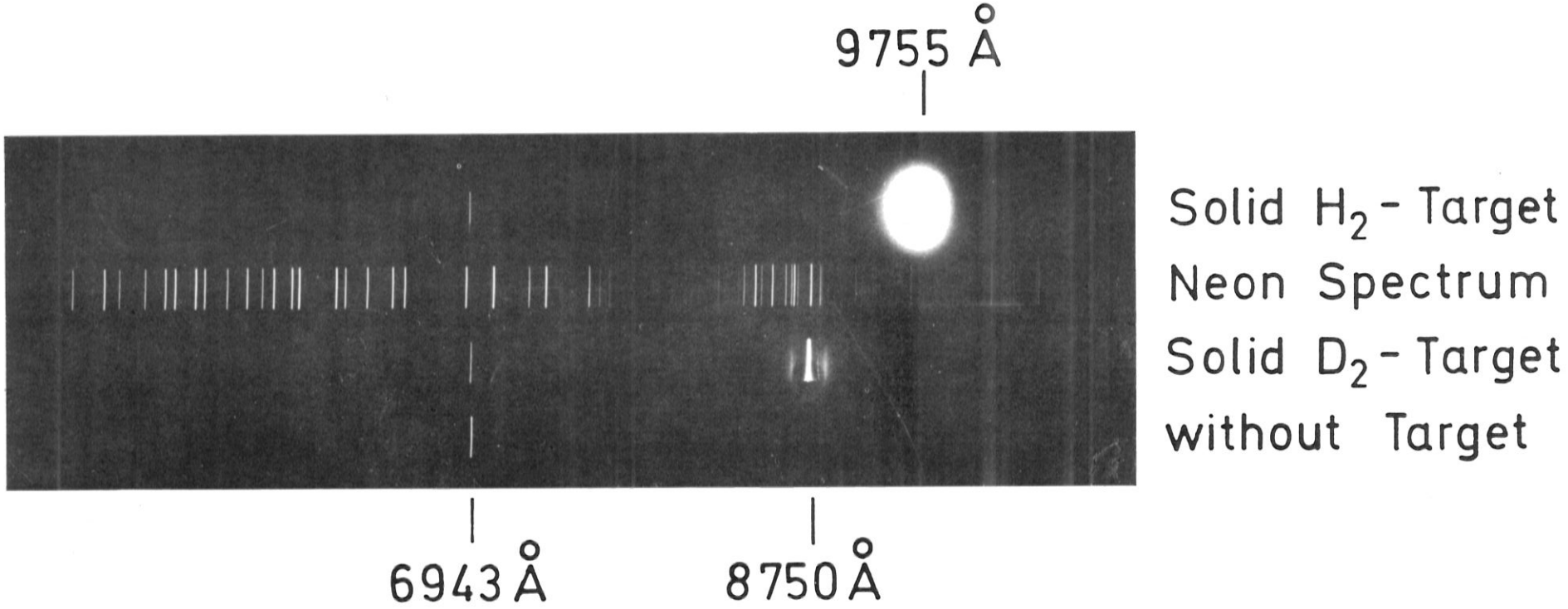

Fig. 7 Spectra of the back-scattered light from a solid hydrogen and solid deuterium target. Irradiation of the target with a ruby laser.

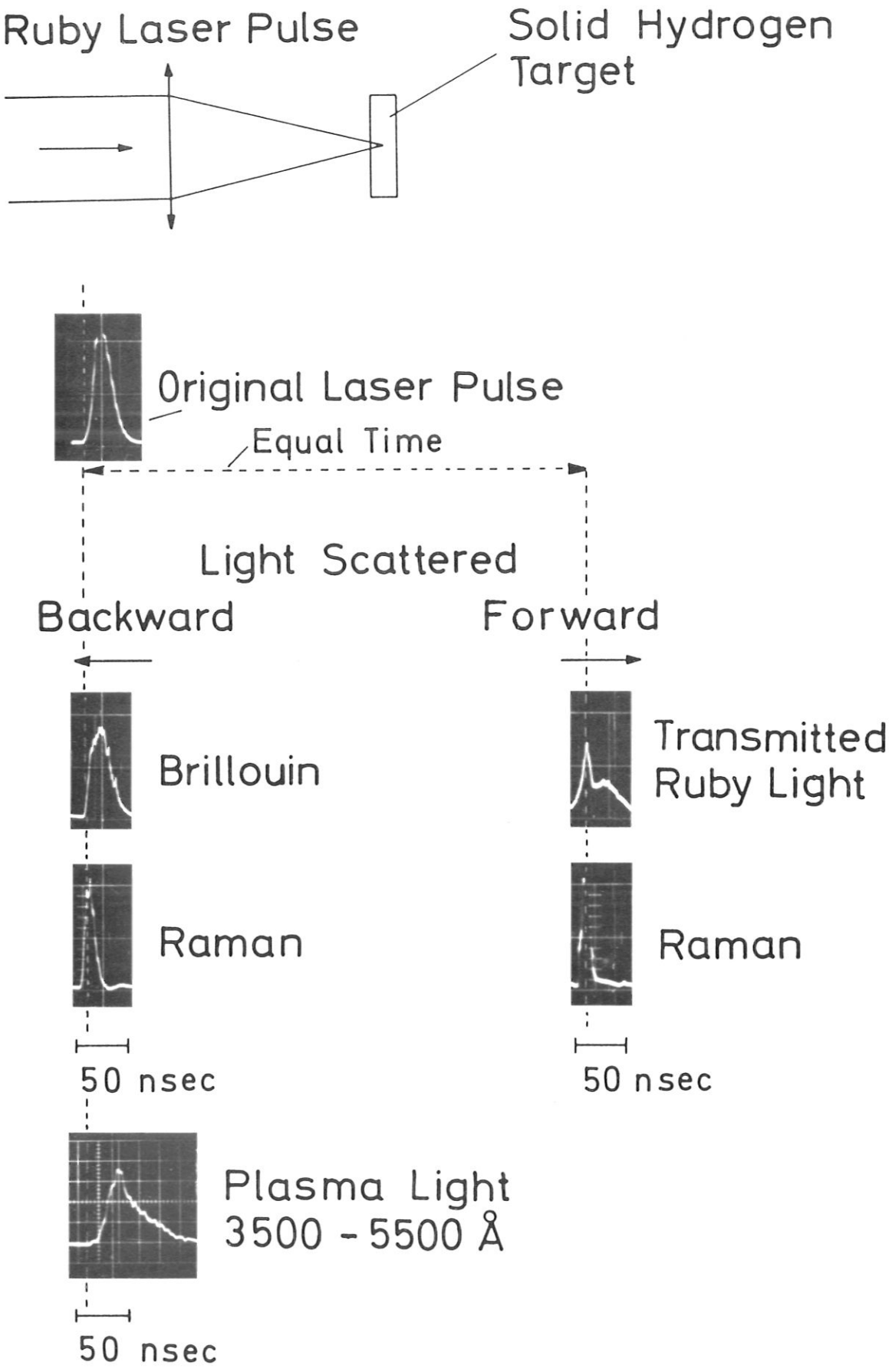

Fig. 8 Time-resolved measurements of Raman-Stokes emission from a solid hydrogen target irradiated by a ruby laser.

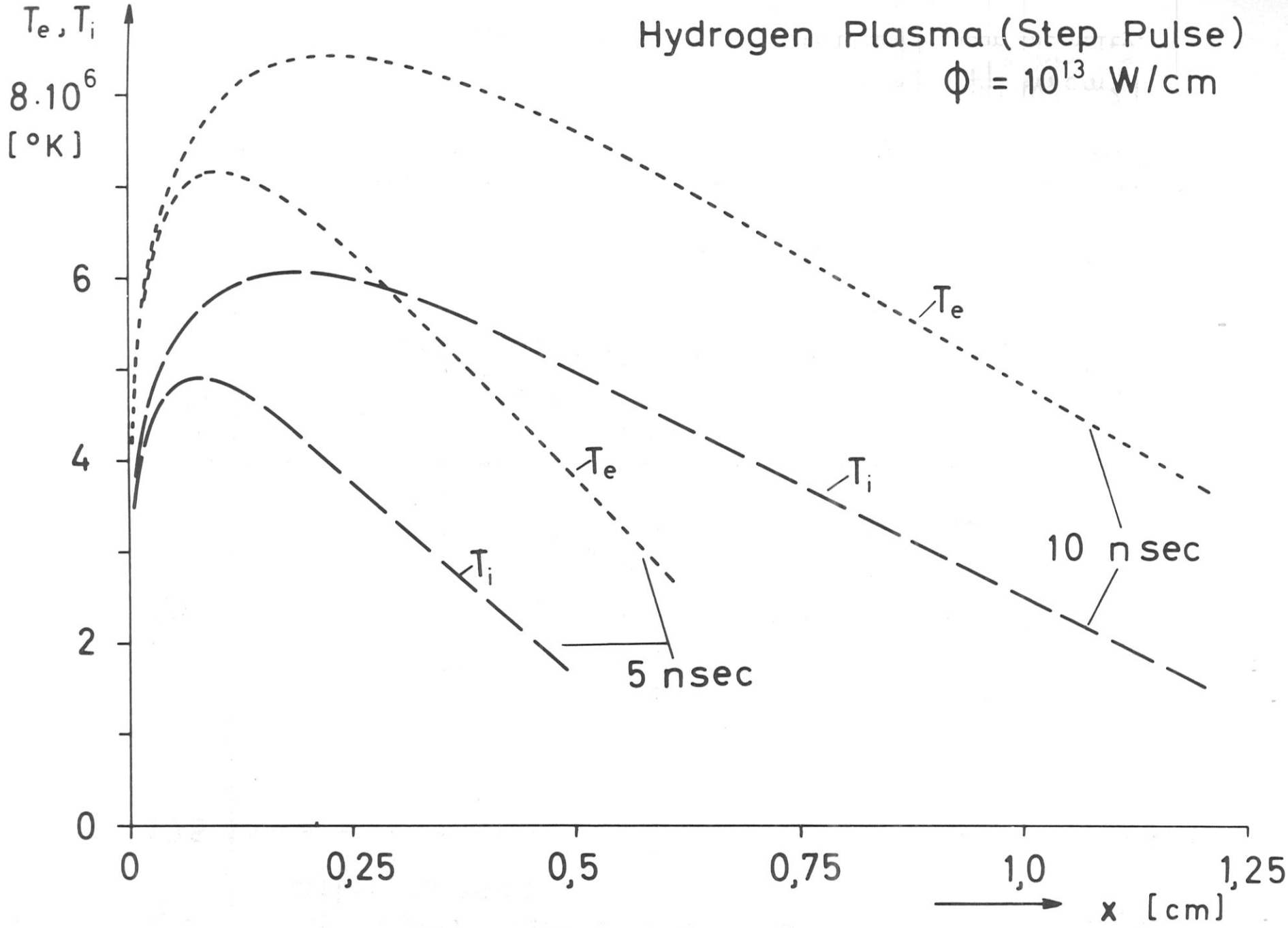

Fig. 9 Profiles of T_e and T_i for a solid hydrogen target. One-dimensional geometry. Target located at x = o.

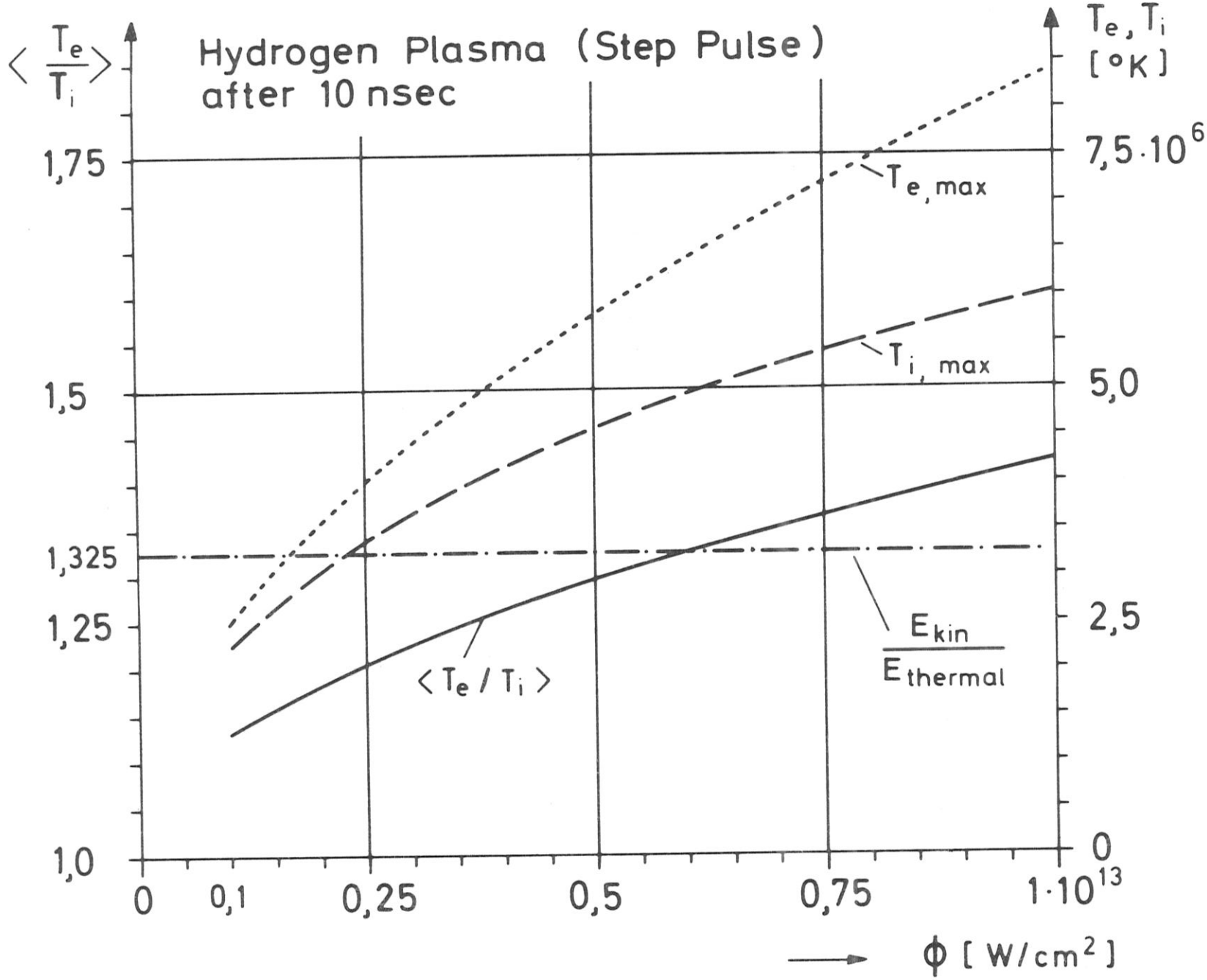

Fig. 1o $T_{e,max}$ and $T_{i,max}$ in the plasma as a function of laser intensity.

Multicomponent Plasma

$$\frac{\partial n_i}{\partial t} + \frac{\partial}{\partial x}(n_i v_i) = 0$$

$$m_i n_i \frac{dv_i}{dt} = -\frac{\partial p_i}{\partial x} + n_i Z_i e E + \sum_{j \neq i} R_{ij}$$

$$0 = -\frac{\partial p_s}{\partial x} - n_e e E$$

$$n_e \frac{d\varepsilon_e}{dt} = \frac{\partial \phi}{\partial x} - p_e \frac{\partial v_e}{\partial x} - \kappa_e \frac{T_e - T_i}{T_e^{3/2}}$$

$$n_i \frac{d\varepsilon_i}{dt} = \kappa_i \frac{T_e - T_i}{T_e^{3/2}} - p_i \frac{\partial v_i}{\partial x}$$

Fig. 11 Set of equations used to describe formation and expansion of a multicomponent plasma.

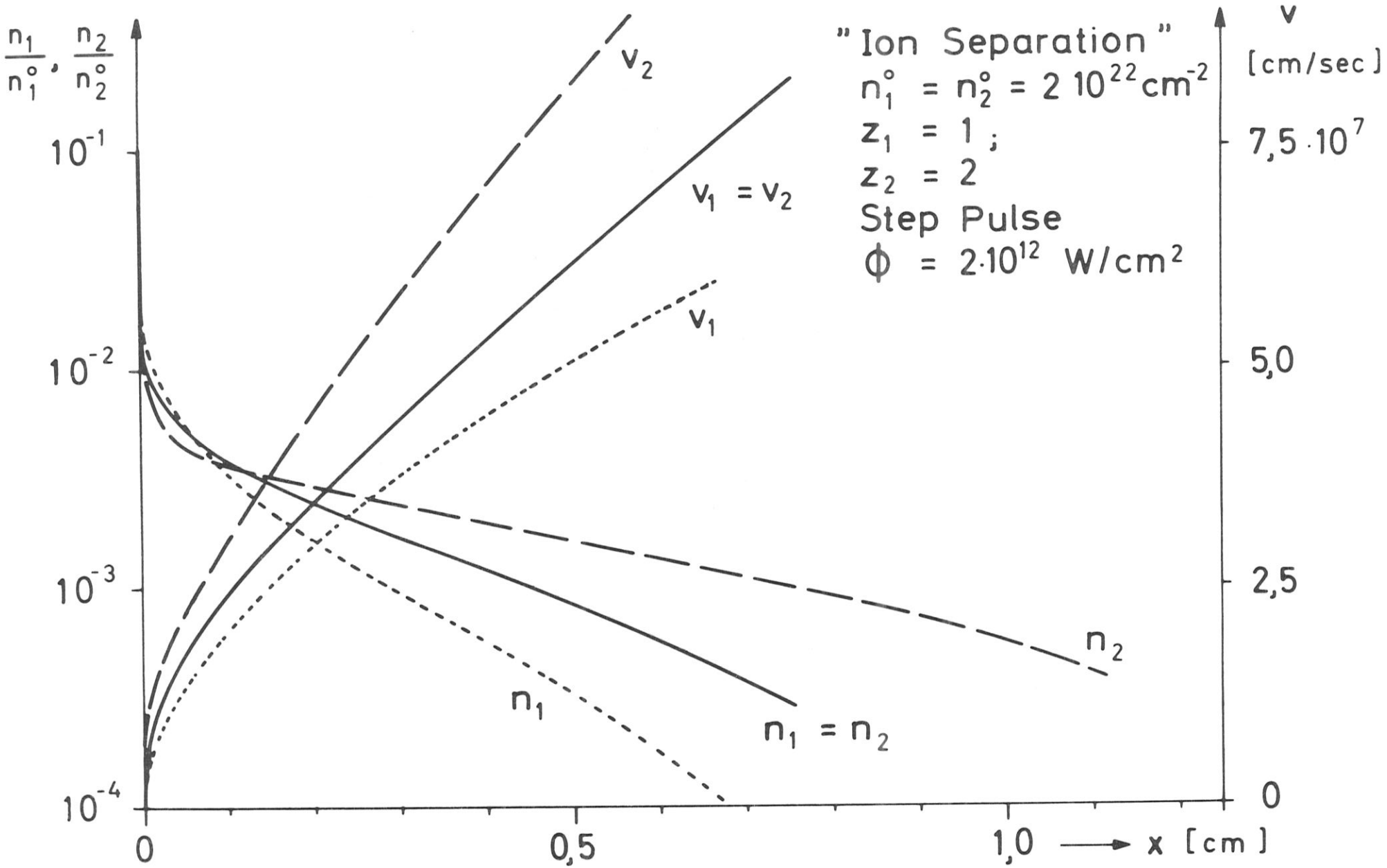

Fig. 12 Profiles of density and velocity for a two-component plasma. Dotted and dusted curved are calculated without friction, solid curves with friction.

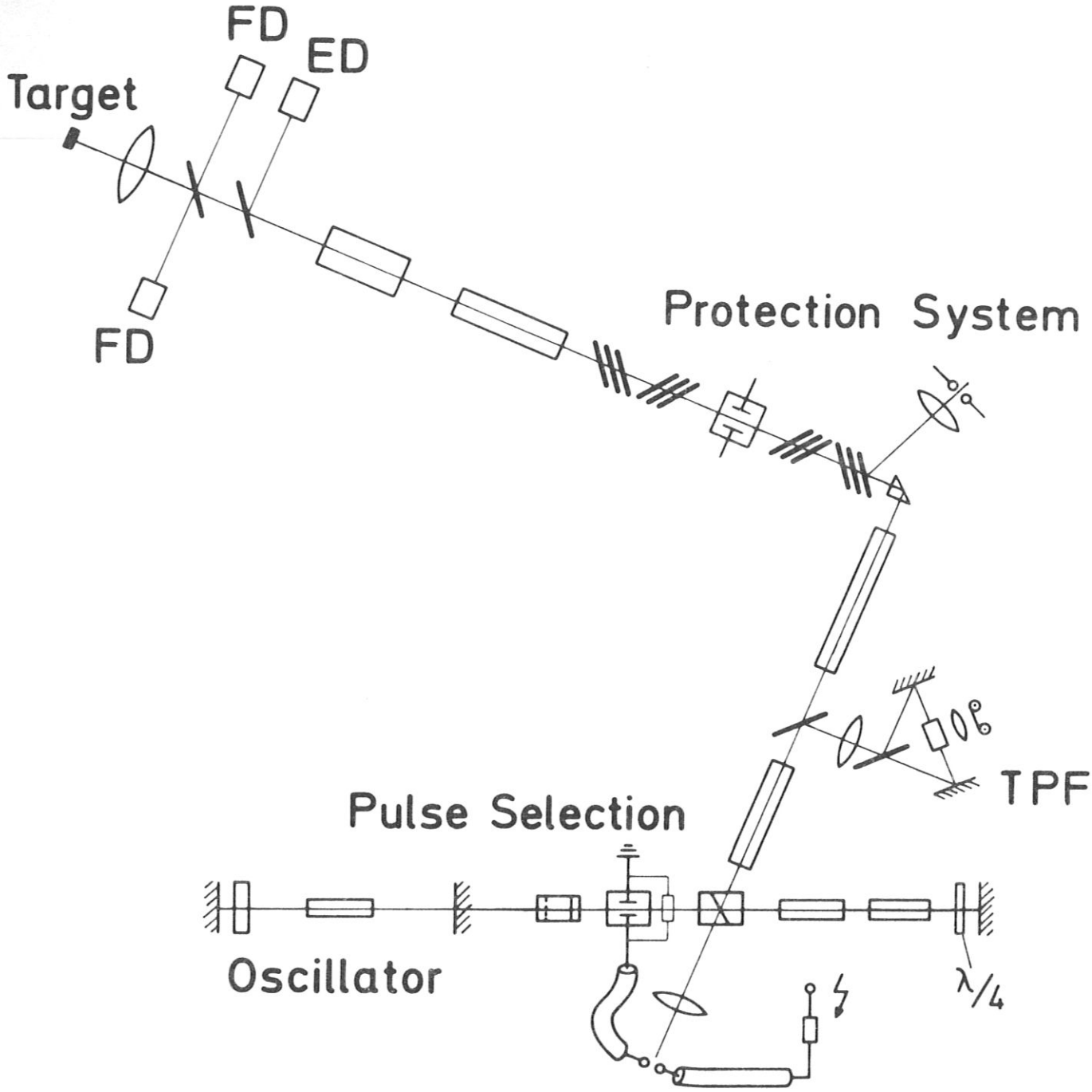

Fig. 13 Plasma production with picosecond laser pulses. Experimental set-up.